*Prion*, 11:431–439, 2017

ISSN: 1933-68961933-690X online
DOI: 10.1080/19336896.2017.1384109



*RESEARCH PAPER*

# Electron microscopic and confocal laser microscopy analysis of amyloid plaques in chronic wasting disease transmitted to transgenic mice

Beata Sikorska[a], Agata Gajos[b], Andrzej Bogucki[b], Emil Zielonka[a], Christina Sigurdson[c], and Pawel P. Liberski[a]

[a]Department of Molecular Pathology and Neuropathology, Medical University of Lodz, Kosciuszki 4 st, Lodz, Poland;
[b]Department of Extrapyramidal Diseases, Medical University of Lodz, Kosciuszki 4 st, Lodz, Poland;
[c]Center for Veterinary Sciences and Comparative Medicine, University of California, San Diego, United States of America

**ABSTRACT.** We report here on the ultrastructure of amyloid plaques in chronic wasting disease (CWD) transmitted to Tg20 transgenic mice overexpressing prion protein ($PrP^c$). We identified three main types of amyloid deposits in mCWD: large amyloid deposits, unicentric plaques similar to kuru plaques in human prion diseases and multicentric plaques reminiscent of plaques typical of GSS. The most unique type of plaques were large subpial amyloid deposits. They were composed of large areas of amyloid fibrils but did not form „star-like" appearances of unicentric plaques. All types of plaques were totally devoid of dystrophic neuritic elements. However, numerous microglial cells invaded them. The plaques observed by confocal laser microscope were of the same types as those analyzed by electron microscopy. Neuronal processes surrounding the plaques did not show typical features of neuroaxonal dystrophy.

**KEYWORDS.** Chronic wasting disease – prion diseases, amyloid plaques – microglial cells

## *INTRODUCTION*

Chronic wasting disease (CWD) is a prion disease occurring naturally in wild and captive mule deer, white-tailed deer, Rocky mountain elk and wild moose. CWD was described as spongiform encephalopathy in deer by Williams and Young[1] and amyloid plaques there

**Correspondence to:** Pawel P. Liberski; Email: ppliber@csk.am.lodz.pl; Medical University of Lodz, Department of Molecular Pathology and Neuropathology, Czechoslowacka st. 8/10, 92-216 Lodz, Poland

by Gajdusek and his coworkers.[2–5] We described early in 1990s the neuropathology of CWD in natural and experimental animals.[6–9] Recently, the first CWD case in free-ranging reindeer (*Rangifer tarandus tarandus*) was diagnosed in southern Norway.[10] Neuropathologically, CWD is characterized by the presence of vacuolated neurons, spongiform change in the neuropil and, mostly in mule deer, by amyloid plaques. Previously we reported on strain fidelity in mouse-adapted CWD.[8] To characterize the inflammatory and neuritic elements adjacent to the amyloid deposits and to compare the amyloid plaques of mCWD to those occurring in other prion diseases we analyzed ultrastructure and three-dimensional structure of amyloid plaques in chronic wasting disease (CWD) transmitted to Tg20 transgenic mice overexpressing prion protein ($PrP^c$).

## MATERIAL AND METHODS

### Mice and inoculum

mCWD was serially propagated in tga20 mice. Here the 5$^{th}$ passage of mCWD in tga20 mice was used. Homogenates from individual animals were used for the inoculation. Tga20 mice were anesthetized with ketamine and xylazine and intracerebrally inoculated into the left parietal cortex with 30 $\mu$l of prion-infected brain homogenate prepared from terminally ill mice. Mice were monitored three times weekly, and TSE was diagnosed according to clinical criteria including ataxia, kyphosis, stiff tail, hind leg clasp, and hind leg paresis. The incubation period was calculated from the day of inoculation to the day of terminal clinical disease.

### Electron microscopy

For electron microscopy, animals were perfused with 4% paraformaldehyde and 1% glutaraldehyde in cacodylate buffer, pH 7.4, postfixed in 1% osmium tetoxide and embedded in Epon. The semithin sections from cerebral (CA1 region) and cerebellar cortices, corpus callosum, hippocampus and the brain stem were selected and stained with toluidine blue. Grids were examined in Jeol 1100 transmission electron microscope.

### Immunohistochemistry

Immunohistochemistry was performed on 4 $\mu$m thick sections of formalin-fixed paraffin embedded blocks. Sections were stained for the following antibodies: anti-prion protein (mouse monoclonal, clone 6H4, 1:400, pretreatment: 98% formic acid, Prionics, Switzerland), anti-Iba1 (rabbit polyclonal, 1:100, pretreatment: citrate buffer pH 6,0; Wako, Japan) and anti-NFP-medium chain (goat polyclonal, 1:100, pretreatment: citrate buffer pH 6,0; Abcam, UK) were used. For visualization EnVision+ System-HRP (Dako, Denmark) was used. Finally, sections were counterstained with haematoxylin.

### Immunofluorescence

For double immunofluorescence stainings, 4% formalin fixed and paraffin-embedded tissues from mice brain were used. Sections were mounted on tissue slides and processed routinely. The sections were then treated with citrate antigen retrieval solution (Target Retrieval Solution 10X Concentrate, pH6.0, Dako). Additionally, the sections were incubated in 98% formic acid. As primary antibodies, anti-Prion Protein (mouse monoclonal, clone 6H4, 1:200, Prionics), anti-CD68 (rabbit polyclonal, 1:50, ProteinTech), anti-Iba1 (rabbit polyclonal, 1:50, Wako), anti-GFAP (rabbit polyclonal, 1:250, Dako) and anti-NFP (rabbit polyclonal, 1:500, ThermoFisher Scientific) were used. The fluorescent-labelled secondary antibodies were Alexa Fluor 488 (donkey anti-mouse, 1:200, Molecular Probes by Life Technologies) and Cy5 (goat anti-rabbit, 1:100, Jackson ImmunoResearch). The following combinations were applied: PrP (AF488)/CD68 (Cy5), PrP (AF488)/GFAP (Cy5), PrP (AF488)/Iba1 (Cy5) and PrP (AF488)/NFP (Cy5). Tissue slides were mounted with Prolong Gold antifade reagent (Molecular Probes by Life Technologies). The stained slides were

evaluated with a confocal laser-scanning microscope (FV1200, Olympus, Japan).

### *Confocal imaging and reconstructions*

Image sizes of 1024 ∼ 1024 pixels were obtained to allow for the greatest spatial discrimination between pixels and maximise resolution potential in the XY dimension. Serial optical sections in the Z dimension were captured to allow for three-dimensional (3D) reconstruction. Imaris software version 8.1.2 (Bitplane AG®, Zurich, Switzerland) was used to generate the 3D reconstructed images. Confocal Z-stacks comprising up to 20 images were reconstructed into 3D animations. Solid skinned cell-surface rendering was using Surface function. The filament tracer mode was used for detection of neurons and astrocytes.

## *RESULTS*

In the 5th passage mice amyloid plaques were present in the corpus callosum, the basal ganglia, the thalamus and the hippocampus but not in the cerebral and cerebellar cortex.

### *Immunohistochemistry*

Immunohistochemical reactions revealed abundant microglial reaction around the amyloid plaques in all areas examined (Fig. 1a). Interestingly we found no dystrophic neurites around the plaques. The neurofilament immunoreactive processes were slightly rearranged in the vicinity of the amyloid deposits, but their morphology was not dystrophic (Fig. 1a). On the other hand, dystrophic neurites were present in subcortical regions and in the brain stem, in a distance from amyloid deposits (Fig. 1b, c).

FIGURE 1A. Amyloid plaque (arrow) in the corpus callosum surrounded by morphologically unchanged neurites. Immunostaining for anti NFP-medium chain, magnification 200x.

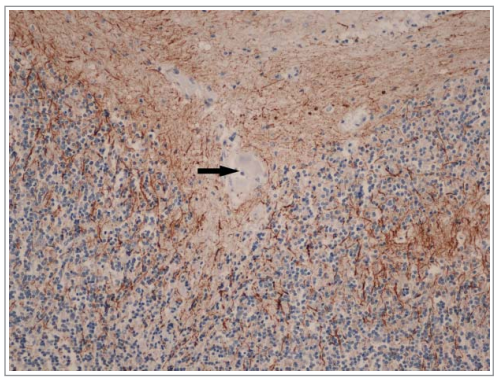

FIGURE 1B. Amyloid plaque in the corpus callosum surrounded by microglial cells. Immunostaining for Iba1, magnification 200x.

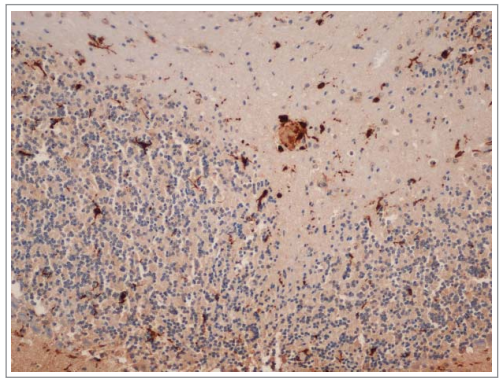

### *Ultrastructure*

Electron microscopy performed on perfusion-fixed brains confirmed our preliminary

FIGURE 1C. Dystrophic neurites in the brain stem. There are no amyloid plaques in proximity. Immunostaining for NFP-medium chain, magnification 400x.

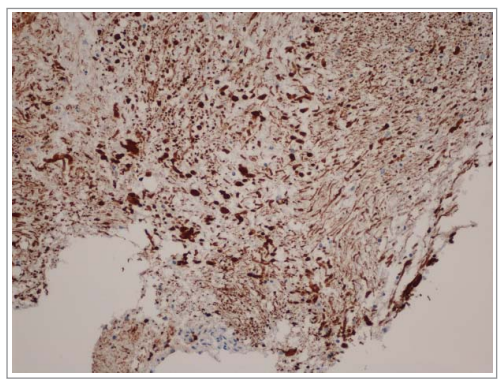

FIGURE 2. Numerous plaques (arrows) in the thalamus. Note the lack of neuritic elements around the plaques; semi-thin section stained with tolouidine blue, x 40.

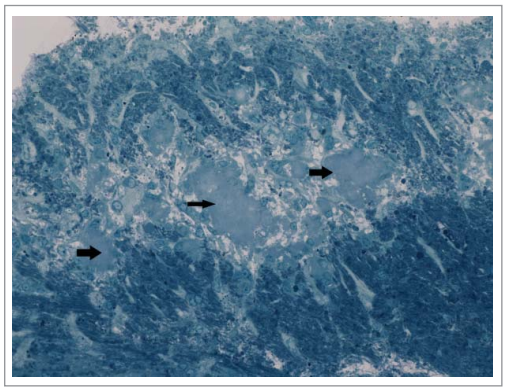

data obtained on material reversed from paraffin blocks to electron microscopy.[8]

As described previously[8] two main types of plaques were present in mCWD: stellate unicentric and large multicentric plaques. However by electron microscopy some of the large plaques did not show the typical morphology of multicentric plaques. Thus by electron microcopy we were able to identify three main types of amyloid deposits in mCWD: large amyloid deposits (Fig. 2, 3), unicentric plaques similar to kuru plaques in human prion diseases (Fig. 4) and multicentric plaques reminiscent of plaques typical of GSS (Fig. 5). Large and multicentric plaques were mainly located subpially while unicentric plaques were observed in the brain

FIGURE 3. A large area totally covered with amyloid fibrils; x 8300.

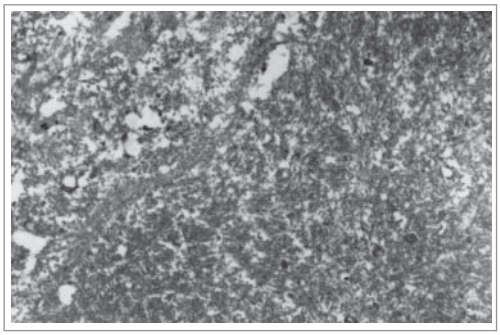

FIGURE 4. An unicentric plaque – "kuru" plaque with a microglial cell (arrows) x 8300.

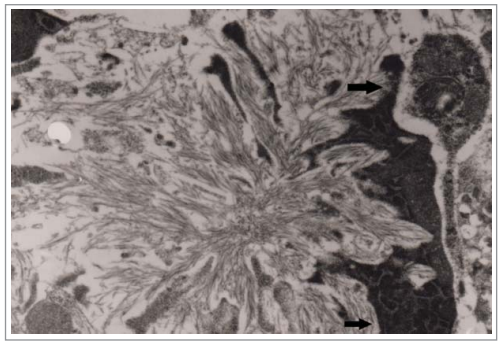

parenchyma and perivascularly (Fig. 4). Ultrastructurally unicentric plaques were composed of bundles of amyloid fibrils deeply interwoven in the centre and radiating toward periphery (Fig. 4, 6). Perivascular plaques were those unicentric kuru plaques that were in close contact with cerebral brain vessels (Fig. 6). In the latter situation, amyloid fibrils were in close contact, or even merged with, with basal membranes. The most unique type of plaques were large subpial amyloid deposits Fig. 3). They were composed of large areas of amyloid fibrils but did not form „star-like" appearances of unicentric plaques. As described previously, all those plaques were totally devoid of dystrophic neuritic elements. However, numerous microglial cells invaded them (Fig. 4, 7a, 7b). Those cells looked very active with enlarged cisterns of

FIGURE 5. Multicentric plaque. Separate cores are marked with arrows; original magnification, x 5000.

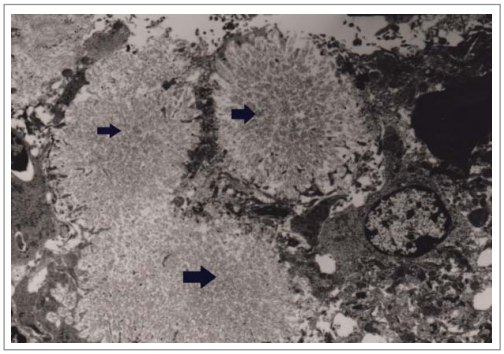

FIGURE 6. Unicentric (kuru plaque; flower symbol) in close contact to the blood vessel (heart symbol). Thin arrows, amyloid fibrils; thick arrows, basal membrane; x 83 000.

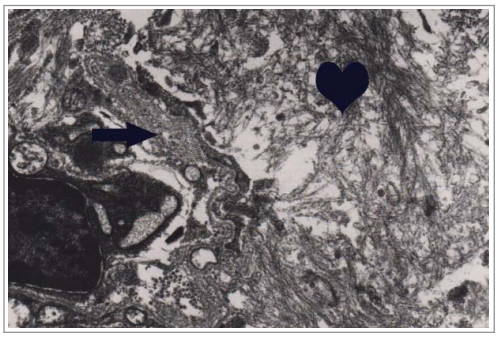

endoplasmic reticulum. The outer membranes formed pockets were amyloid fibrils seemed to be „engulfed" (Fig. 5). Some cells were very dense and contained amorphous masses of even higher density. The labyrinth-like network of microglial processes was visible at the periphery and within plaques.

### *Confocal laser microscopy*

Using confocal microscopy and three-dimensional image analysis software (Imaris Version 8.2, Bitplane AG, Switzerland) we were able to study the structure of the amyloid plaques, their spatial organization and association with glial and neuronal cells. To obtain a more quantitative view of astrocytic and neuronal processes, processes were reconstructed as three-dimensional skinned models and measured using both Imaris automatic tracing and manual tracing. The plaques observed by confocal laser microscope were of the same types as those analyzed by electron microscopy: unicentric, multicentric and perivascular or large subpial amyloid deposits. In the brain sections that were double stained for PrP and neurofilament proteins, we recognized neuronal processes surrounding the plaques or, to some extent, intermingled with the amyloid fibres within the plaque (Fig. 8 and 9). Interestingly, the axons did not show typical features of neuroaxonal dystrophy such as swellings or

FIGURE 7. (a) Amyloid plaques (envelope) surrounded by microglial cells (arrows); original magnification, x 8300; (b) Amyloid fibrils (flower) in close contact with activated microglial cell (arrow); x 13 000.

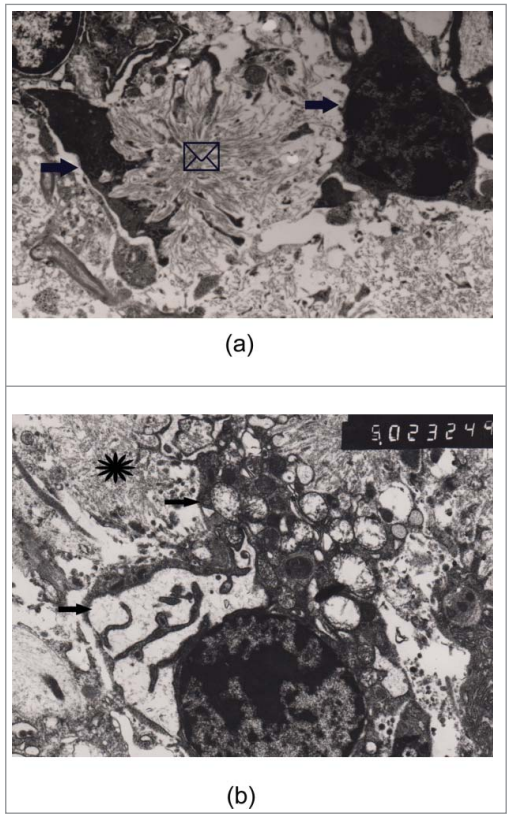


distortion, independently of the plaque type. In the brain sections double stained for the astroglial marker – GFAP and PrP, we observed astrogliosis with astrocytes surrounding and embracing the amyloid plaques but the processes of glial cells hardly entered the plaques. In all types of plaques double staining for microglia (Iba1) and PrP showed prominent microglial reaction around the plaques. The microglia were tightly enfolding the plaques with their processes deeply invading the interior of the plaque (Fig. 10).

## *DISCUSSION*

We reported here on brain amyloid plaques in transgenic mice infected with CWD. Some

FIGURE 8. Large subpial multicentric amyloid plaque surrounded by neuronal processes. Confocal laser microscopy, prion protein (6H4) — green, neurofilaments — red, magnification 600x, digital zoom 2.1x. Three-dimensional reconstruction of neuronal morphology by filament tracing software.

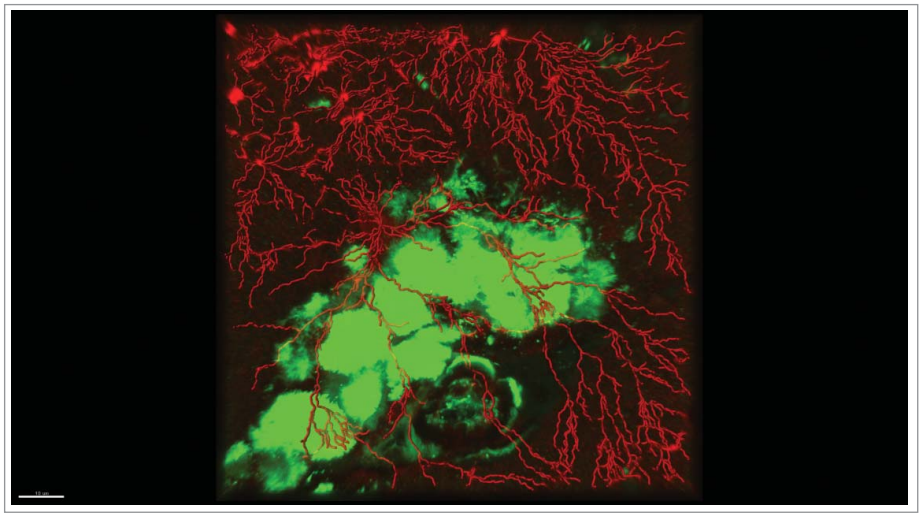

of these plaques are reminiscent of other types of plaques described in prion diseases, however some as large amyloid deposits are not observed in other prion diseases.

In human prion diseases, plaques occur always in kuru,[11] in Gerstmann-Straussler-Scheinker (GSS) disease, variant CJD[12] and in a certain proportion of sporadic and iatrogenic Creutzfeldt-Jakob disease.[12,13,14] In kuru, plaques are very similar to unicentric plaques described here but contained sparse dystrophic neurites.[12] Interestingly, in captive mule deer CWD unicentric plaques also contained dystrophic neurites, but in Tg mice infected with

FIGURE 9. The same amyloid plaque surrounded by neuronal processes. Confocal laser microscopy, prion protein (6H4)-green, neurofilaments — red, magnification 600x, digital zoom 2.1x. Three-dimensional reconstruction of neuronal morphology and amyloid by filament tracing software.

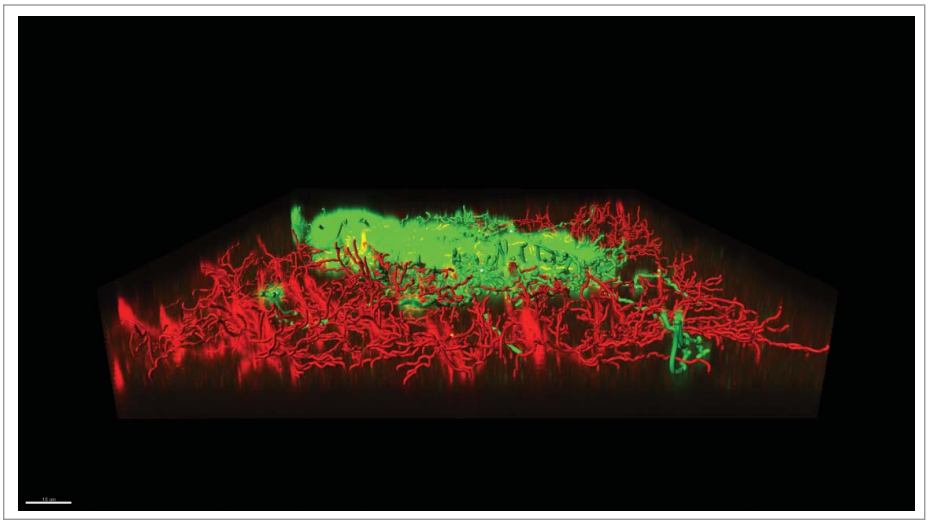

FIGURE 10. Amyloid unicentric plaque surrounded by microglial cells. Confocal laser microscopy, prion protein (6H4) — green, microglial cells (Iba1) — red, magnification 400x, digital zoom 1.8x.

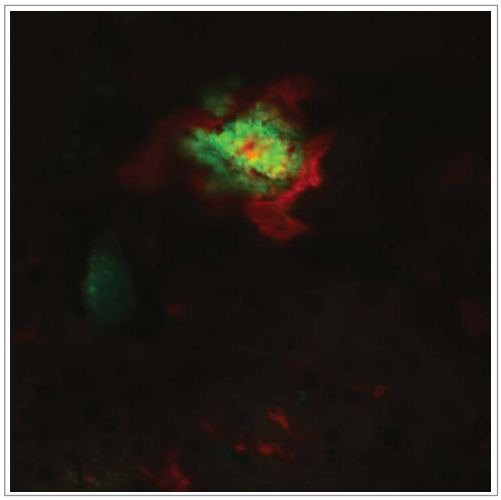

CWD there are no dystrophic neurites around amyloid deposits.[6] Dystrophic neurites are degenerating dendrites or axonal terminals and preterminals which accumulate autophagic vacuoles and lysosomal electron-dense bodies. Those subcellular organelles are visible only by electron microscopy and should form a basis for definition of dystrophic neuritis. However, on a basis of correlative studies using light- and electron microscopy, this definition was extended to cover bulbs and rings observed at the light microscopy level.[15] Dystrophic neurites are abundant in Alzheimer disease (AD), another protein-misfolded disease[16] where a-beta peptide amyloid spreads in prion-like fashion.[17] A caveat, what comes first - amyloid or neuroaxonal dystrophy seems solved by two-photon in vivo studies[18] using young APPswe/PS1d9xYFP (B6C3-YFP) mice. In these mice plaques develop fast followed by dystrophic neurites. Our studies using transmission electron microscopy also showed that unicentric plaques are not neuritic and neurites do not invade but bypass the plaque as evidenced by image reconstruction of confocal microscopy. This study adds to the evidence that the plaques develop and dystrophic neurites can develop in response to certain types of plaques only.

Since our first description of microglia in plaques of GSS,[19] these cells became a target of intensive research. The basic tenet of this research is to answer the question on the role of microglia; are they a producer or just a scavenger of amyloid.[20] In mice with a disrupted gene for a microglial receptor Cx3cr1,[21] inoculated with 3 different strains of scrapie and BSE, the incubation period was shortened while the neuropathology pattern and microglia activation remained unaltered.

In conclusion, we reported here the diversity of PrP-amyloid deposits encountered in CWD – infected Tg20 mice. Generally, we confirmed the presence of abundant amyloid plaques in CWD-infected Tg20 samples reversed from paraffin blocks[8] and those published by us in captive mule deer.[6,9] However, large amyloid deposits were observed for the first time.

Numerous microglial processes were visible within the plaques and at the periphery of plaques. The latter was particularly evident in unicentric deposits, a phenomenon described by us and the others in Gerstmann-Straussler-Scheinker disease (GSS) a quarter of century earlier,[19,22,23] but also in florid plaques in vCJD and kuru plaques in kuru.[12] Microglia are derived from c-kit+ erythromyeloid precursor in the yolk sac.[24] The role of microglia in prion disease is unclear. It seems that they are infectious[25] and exhibit unique profile of RNAs typical for inflammatory disease.[26] They are readily observed in CJD[27] and in scrapie[28] and the intensity of microglial activation is dependent on the molecular type of PrP aggregate.[29] The presence of type 1 of PrP peptide correlates with abundance of CR3/43-immunostained microglia while the presence of the type 2 peptide not. In cases with both peptides present, the regional enhancement of microglia reaction correlates with the presence of peptide 1 of PrP. The exact role of microglia is not that clear[30] and it has been even suggested that microglia may play a neuroprotective role in prion diseases.[30]

Alzheimer disease another neurodegenerative disease, also characterized by abundant plaque formation, is recently classified as "prion-like disease".[16,31] The induction of amyloid beta plaques in cadaver died with CJD

following dura matter transplantation strongly suggests the prion-like mechanism.[17,20,32,33]

To sum up, we described here a range of amyloid deposits in CWD passaged through Tg20 transgenic animals. These deposits recapitulate those observed in naturally occurring CWD in mule deer but they are devoid of dystrophic neurites. In contrast in human prion diseases amyloid plaques are surrounded by numerous (GSS, vCJD) or sparse (sCJD, kuru) dystrophic neurites. Both electron microscopy and confocal laser microscopy showed numerous microglial processes within the plaques and at the periphery of plaques in mCWD.

## *ACKNOWLEDGMENTS*

Professor James W. Ironside is kindly acknowledged for helpful criticism. Ryszard Kurczewski, Leokadia Romanska, Elzbieta Naganska and Anna Zielinska are acknowledged for skilfull technical assistance and Ewa Skarzynska for exquisite secretarial assistance and corrections.

This work was supported by the National Science Centre Poland under Grant UMO-2012/04/M/NZ4/00232.

## *FUNDING*

The National Science Center Poland ID: UMO-2012/04/M/NZ4/00232, Principal Investigator: Pawel P. Liberski, ppliber@csk.am.lodz.pl

## REFERENCES

1. Williams ES, Young S. Chronic wasting disease of captive mule deer: a spongiform encephalopathy. J Wildl Dis. 1980;16(1):89–98. doi:10.7589/0090-3558-16.1.89.
2. Bahmanyar S, Williams ES, Johnson FB, et al. Amyloid plaques in spongiform encephalopathy of mule deer. J Comp Pathol. 1985;95(1):1–5. doi:10.1016/0021-9975(85)90071-4.
3. Guiroy DC, Williams ES, Yanagihara R, et al. Topographic distribution of scrapie amyloid-immunoreactive plaques in chronic wasting disease in captive mule deer (Odocoileus hemionus hemionus). Acta Neuropathol. 1991;81(5):475–8. doi:10.1007/BF00310125.
4. Guiroy DC, Williams ES, Yanagihara R, et al. Immunolocalization of scrapie amyloid (PrP27-30) in chronic wasting disease of Rocky Mountain elk and hybrids of captive mule deer and white-tailed deer. Neurosci Lett. 1991;126(2):195–8. doi:10.1016/0304-3940(91)90552-5.
5. Guiroy DC, Williams ES, Song KJ, et al. Fibrils in brain of Rocky Mountain elk with chronic wasting disease contain scrapie amyloid. Acta Neuropathol. 1993;86(1):77–80. doi:10.1007/BF00454902.
6. Guiroy DC, Williams ES, Liberski PP, et al. Ultrastructural neuropathology of chronic wasting disease in captive mule deer. Acta Neuropathol. 1993;85(4):437–44. doi:10.1007/BF00334456.
7. Guiroy DC, Liberski PP, Williams ES, et al. Electron microscopic findings in brain of Rocky Mountain elk with chronic wasting disease. Folia Neuropathol. 1994;32(3):171–3.
8. Sigurdson CJ, Manco G, Schwarz P, et al. Strain fidelity of chronic wasting disease upon murine adaptation. J Virol. 2006;80(24):12303–11. doi:10.1128/JVI.01120-06.
9. Liberski PP, Guiroy DC, Williams ES, et al. Deposition patterns of disease-associated prion protein in captive mule deer brains with chronic wasting disease. Acta Neuropathol. 2001;102(5):496–500.
10. Benestad SL, Mitchell G, Simmons M, et al. First case of chronic wasting disease in Europe in a Norwegian free-ranging reindeer. Vet Res 2016;47(1):88. doi:10.1186/s13567-016-0375-4.
11. Liberski PP, Sikorska B, Lindenbaum S, et al. Kuru: genes, cannibals and neuropathology. J Neuropathol Exp Neurol. 2012;71(2):92–103. doi:10.1097/NEN.0b013e3182444efd.
12. Sikorska B, Liberski PP, Sobów T, et al. Ultrastructural study of florid plaques in variant Creutzfeldt-Jakob disease: a comparison with amyloid plaques in kuru, sporadic Creutzfeldt-Jakob disease and Gerstmann-Sträussler-Scheinker disease. Neuropathol Appl Neurobiol. 2009;35(1):46–59. doi:10.1111/j.1365-2990.2008.00959.x.
13. Krücke W, Beck E, Vitzthum HG. Creutzfeldt-Jakob disease. Some unusual morphological features reminiscent of kuru. Z Neurol. 1973;206(1):1–24.
14. Liberski PP, Sikorska B, Hauw JJ, et al. Ultrastructural characteristics (or evaluation) of Creutzfeldt-Jakob disease and other human transmissible spongiform encephalopathies or prion diseases. Ultrastruct Pathol. 2010;34(6):351–61. doi:10.3109/01913123.2010.491175.
15. Brendza RP, O'Brien C, Simmons K, et al. PDAPP; YFP double transgenic mice: a tool to study amyloid-beta associated changes in axonal, dendritic, and synaptic structures. J Comp Neurol 2003;456(4):375–383. doi:10.1002/cne.10536.

16. Prusiner SB. Biology and genetics of prions causing neurodegeneration. Annu Rev Genet. 2013;47:601–23. doi:10.1146/annurev-genet-110711-155524.
17. Jaunmuktane Z, Mead S, Ellis M, et al. Evidence for human transmission of amyloid-$\beta$ pathology and cerebral amyloid angiopathy. Nature. 2015;525 (7568):247–50. doi:10.1038/nature15369.
18. Meyer-Luehmann M, Spires-Jones TL, Prada C, et al. Rapid appearance and local toxicity of amyloid-beta plaques in a mouse model of Alzheimer's disease. Nature. 2008;451(7179):720–4. doi:10.1038/nature06616.
19. Barcikowska M, Liberski PP, Boellaard JW, et al. Microglia is a component of the prion protein amyloid plaque in the Gerstmann-Sträussler-Scheinker syndrome. Acta Neuropathol. 1993;85(6):623–7. doi:10.1007/BF00334672.
20. Jung CK, Keppler K, Steinbach S, et al. Fibrillar amyloid plaque formation precedes microglial activation. PLoS One. 2015;10(3):e0119768. doi:10.1371/journal.pone.0119768.
21. Grizenkova J, Akhtar S, Brandner S, et al. Microglial Cx3cr1 knockout reduces prion disease incubation time in mice. BMC Neurosci. 2014;15:44. doi:10.1186/1471-2202-15-44.
22. Miyazono M, Iwaki T, Kitamoto T, et al. A comparative immunohistochemical study of Kuru and senile plaques with a special reference to glial reactions at various stages of amyloid plaque formation. Am J Pathol. 1991;139(3):589–98.
23. Liberski PP, Budka H. Ultrastructural pathology of Gerstmann-Sträussler-Scheinker disease. Ultrastruct Pathol. 1995;19(1):23–36. doi:10.3109/01913129509014600.
24. Alliot F, Godin I, Pessac B. Microglia derive from progenitors, originating from the yolk sac, and which proliferate in the brain. Brain Res Dev Brain Res. 1999;117 (2):145–52. doi:10.1016/S0165-3806(99)00113-3.
25. Baker CA, Martin D, Manuelidis L. Microglia from Creutzfeldt-Jakob disease-infected brains are infectious and show specific mRNA activation profiles. J Virol. 2002;76(21):10905–13. doi:10.1128/JVI.76.21.10905-10913.2002.
26. Baker CA, Manuelidis L. Unique inflammatory RNA profiles of microglia in Creutzfeldt-Jakob disease. Proc Natl Acad Sci U S A. 2003;100(2):675–9. doi:10.1073/pnas.0237313100.
27. v Eitzen U, Egensperger R, Kösel S, et al. Microglia and the development of spongiform change in Creutzfeldt-Jakob disease. J Neuropathol Exp Neurol. 1998;57(3):246–56. doi:10.1097/00005072-199803000-00006.
28. Song PJ, Barc C, Arlicot N, et al. Evaluation of prion deposits and microglial activation in scrapie-infected mice using molecular imaging probes. Mol Imaging Biol. 2010;12(6):576–82. doi:10.1007/s11307-010-0321-1.
29. Puoti G, Giaccone G, Mangieri M, et al. Sporadic Creutzfeldt-Jakob disease: the extent of microglia activation is dependent on the biochemical type of PrPSc. J Neuropathol Exp Neurol. 2005 Oct;64 (10):902–9. doi:10.1097/01.jnen.0000183346.19447.55.
30. Zhu C, Herrmann US, Falsig J, et al. A neuroprotective role for microglia in prion diseases. J Exp Med. 2016;213(6):1047–59. doi:10.1084/jem.20151000.
31. Watts JC, Condello C, Stöhr J, et al. Serial propagation of distinct strains of A$\beta$ prions from Alzheimer's disease patients. Proc Natl Acad Sci U S A. 2014;111 (28):10323–8. doi:10.1073/pnas.1408900111.
32. Frontzek K, Lutz MI, Aguzzi A, et al. Amyloid-$\beta$ pathology and cerebral amyloid angiopathy are frequent in iatrogenic Creutzfeldt-Jakob disease after dural grafting. Swiss Med Wkly. 2016;146:w14287. doi:10.4414/smw.2016.14287.
33. Kovacs GG, Lutz MI, Ricken G, et al. Dura mater is a potential source of A$\beta$ seeds. Acta Neuropathol. 2016;131(6):911–23. doi:10.1007/s00401-016-1565-x.